# Experimental study on the seismic behavior in the connection between CFRT column and steel beam

Xilin Lu† and Yong Yu‡

*Tongji University, Shanghai, 200092, China*

Tanaka Kiyoshi† and Sasaki Satoshi‡

*Technical Research Institute of Fujita Corporation, Japan*

**Abstract.** The structural behavior of connections between concrete-filled rectangular tubular column (CFRT column) and steel beam has been studied in this paper through sub-assemblage loading tests. It is found that the sub-assemblages exhibit ductile restoring force characteristics under seismic loading. A formula for the prediction of the yield strength of each member in the connection is proposed by using the yield line theory under the assumption of a simple stress transfer mechanism. It is shown that the proposed formula can produce a reasonable prediction while providing a basis for further investigation.

**Key words:** experiment; seismic behavior; connection; concrete-filled rectangular tubular column; steel beam.

## 1. Introduction

Concrete-filled steel rectangular tubular (CFRT) columns have become increasingly popular in structural applications. This is partly due to their excellent earthquake resistant properties such as high strength, high ductility, and large energy absorption capacity. This enhancement in structural properties depends on the composite action between the constituent materials, while the confinement created by the steel casing may strengthen the material properties of the concrete by putting the concrete into a triaxial state of stress. Conversely, inward buckling of the steel tube is resisted by the infilled concrete; thus the stability and strength of the whole column will increase as a result. Usually, CFRT columns have better structural behavior and higher fire resistance because of the composite action in comparison with hollow rectangular tubular columns (Sasaki *et al*. 1995, Hideto *et al*. 1994, Tie 1996). Therefore, they are increasingly used for high-rise buildings in Japan and other countries. However, this is not the case in China because very few experimental studies on the inelastic behavior of CFRT columns under cyclic loading are available, especially on the connections between a CFRT column and a steel beam or R.C. beam. Thus, further experimental investigations on the behavior of such columns and connections under severe earthquake conditions are necessary in order to develop a reliable earthquake-resistant design method for CFRT structures.

The present study is initiated with the aim of developing a rigid connection with higher shear

---

† Professor
‡ Lecturer

resistance in the joint panel and higher ductility, as compared to a commonly designed one with hollow steel sections. For this purpose, five sub-assemblage specimens were prepared and then tested. In the test, the column was loaded first with a constant value of axial load and then both ends of the beam were subjected to cyclic loading. In the specimen design, an inner diaphragm with circular opening was used to reinforce the rigid beam-to-column connection. The test results are discussed in the light of improvement of strength, ductility and energy-absorption capacity in the connections.

## 2. Outline of experiments

### 2.1. Test specimen

In the present work, five 1/3-scale specimens were designed. The specimens consisted of CFRT columns and steel I-girders rigidly framed into the column. Cross-section properties and geometrical configurations of the specimens are listed in Table 1 and Fig. 1, respectively. The story height ($H$) was 1360 mm and span length ($L$) was 2200 mm. Four specimens consisted of concrete-filled steel tubulars with a square section, and the other one was without infilled concrete. The section of steel column was fabricated by a full-penetration welding at every corner seam. Columns are of square cross-section with a 300 mm width, and the shear span length ($L_C$) was 550 mm. The beam was

Table 1 Cross-section properties and axial load on columns

| Specimen No. | Hollow section of column $B_c \times D_c \times t_{cf}$ (mm) | Beam section $H_b \times B_b \times b_{bw} \times t_{bf}$ (mm) | Diaphragm thickness $t_j$ (inner diameter) (mm) | Axial load $N$ (kN) | Concrete grade |
|---|---|---|---|---|---|
| YG1 | □ -200 × 200 × 5 | BH-260 × 100 × 5 × 5 | 6 (Φ70) | $0.2N_0$ (200) | None |
| YG2 | □ -200 × 200 × 5 | BH-260 × 100 × 5 × 5 | 6 (Φ70) | $0.2N_0$ (450) | C40 |
| YG3 | □ -200 × 200 × 5 | BH-260 × 100 × 5 × 5 | 6 (Φ70) | $0.4N_0$ (1000) | C50 |
| YG4 | □ -200 × 200 × 4 | BH-260 × 100 × 5 × 5 | 6 (Φ70) | $0.2N_0$ (420) | C40 |
| YG5 | □ -200 × 200 × 4 | BH-260 × 100 × 5 × 5 | 6 (Φ70) | $0.4N_0$ (900) | C50 |

Note: $N_0 = f_y \cdot A_s + f_c \cdot A_c$
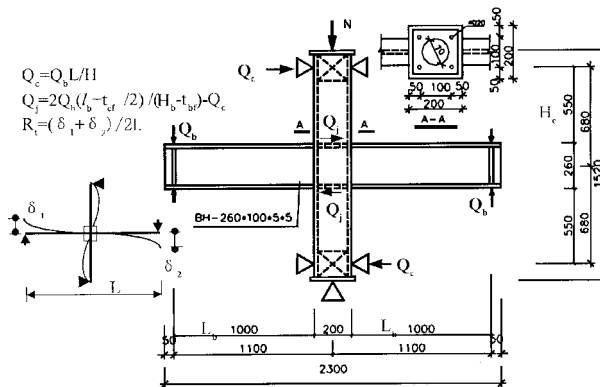


Fig. 1 Configuration of specimens

Table 2 Material properties
(a) Steel

| Steel plate thickness (mm) | Measured thickness (mm) | Yield point (MPa) | Tensile strength (MPa) | $E_s$ (MPa) | Elongation (%) |
|---|---|---|---|---|---|
| 4 | 4.1 | 250 | 419 | 200800 | 36.0 |
| 6 | 6.2 | 230 | 414 | 201000 | 34.5 |
| 5 | 4.9 | 240 | 415 | 199100 | 30.5 |

(b) Concrete

| Concrete grade | $f_{CU}$ (MPa) | $f_C$ (MPa) | $E_C$ (MPa) | Age (days) |
|---|---|---|---|---|
| C40 | 37 | 33 | 30200 | 124 |
| C50 | 43 | 39 | 31000 | 124 |

also fabricated by welding. Distance from loading point on the beam to the column face ($L_b$) was 1000 mm. Two horizontal diaphragms reinforced the beam to column connections with circular holes for all the specimens, and the diaphragms were connected to column walls by a full-penetration welding. As shown in Table 1, the test parameters of the CFRT specimens are as follows: (a) the width-to-thickness ratio of the square hollow section; (b) the concrete grade; (c) the constant axial load applied on the column. The mechanical properties of steel and concrete are shown in Table 2(a) and Table 2(b), respectively.

The strain gauges were attached onto the beam flange, the beam web and the column wall to inspect the yielding of the beam and the column. And on the joint zones between the column and the beam, there were several LVDTs mounted diagonally on the column walls, to measure the shear deformation within the joint.

To simulate the seismic loading condition, specimens were tested under anti-symmetric incremental cyclic reversal loading on both ends of the beam with constant axial load ($N/N_0$) on the column. The anti-symmetric beam shear force $Q_b$ was varied to obtain increasing increments of story drift rotation $R_t$ which equals to 5, 10, 20, 30, $40 \times 10^{-3}$ radians, respectively. For each rotation increment, two full-cycles of loading were performed. Force, displacement and strain in each member were measured during the testing.

## 2.2. Test results

### 2.2.1. Failure modes

It is believed that the failure procedures of the specimens are useful in understanding their load-deformation behavior. Therefore, in this section, phenomena observed during the tests will be described in detail.

For all the specimens, local buckling was first observed in the flange of the steel beam nearest to the joint zone before the peak load. Once local buckling occurred, the flange plates were no longer fully straightened out during reversed loading. As the load was increased, the buckling deformation progressively grew, and eventually the specimen lost its resistant capacity, with the occurrence of vertical cracking in the beam flange and web or in the occurrence of considerable fracture in the column tube.

For specimen YG1, there was no concrete filled in the steel tubular column but two diaphragms

were provided in the joint zone. Similar to other specimens, initial buckling occurred at the flanges of the beam nearest to the joint zone. As the loading continued, the flange of the column slightly buckled outward in the position corresponding to the tension flange of the steel beam. No obvious buckling deformation was found in the compressive part of column flange corresponding to the compression flange of the beam. This is because the inner diaphragm resists the buckling of plates toward the inner direction. Just before the peak load, a sudden sound caused by a fracture of the steel plate from the joint zone was heard, and then a rapid deterioration in the strength was observed. At the same time, the outward buckling deformation of the column flange increased sharply because tension in the beam flange resulted in the tube wall separations from the inner diaphragm. Cracking on the tube wall was observed at the junction between the flange of the beam and that of the column. The test was terminated when the crack width on tube wall was as large as 3 cm. The joint zone was opened by gas cutting after test, and it was observed that the welding between the inner diaphragm and the column flange had been destroyed.

The same failure mode was observed in the test of specimen YG2. However, this time the fracture of welding of the inner diaphragm occurred later and the outward buckling deformation of the column flange was smaller as compared to specimen YG1. This is probably due to the composite action caused by the infilled-concrete. Prior to fracture in the welding of the diaphragm, these two specimens exhibited a quite stable inelastic behavior. Unfortunately an unexpected failure mode took place and satisfactory performance was observed only up to a drift of about 2%. The occurrence of this kind of fracture in the welding area might have resulted from poor welding quality or a low-cycle fatigue. Therefore, special attention must be paid to the welding of the inner diaphragm in practical construction.

For specimens YG3~YG5, the local buckling deformation of the beam's flanges was dominant in comparison with that of the column flange during the whole test. Initial buckling in the beam flanges appeared when the story drift was around 1.5%, which corresponded to 80~90% of the ultimate strength. As displacement history of the loading increased, the local buckling of the beam flanges became more and more conspicuous so it was very difficult to control the displacement manually. Partly for this reason, no significant post-yield stiffness or strength deterioration was observed prior to the ultimate failure of the connections. These connections were clearly able to develop the plastic bending strength of the steel beams. Ultimate failure of these connections was due to the fracture of the beam flange in the connection stub region. This fracture was relatively abrupt, and eventually propagated into the web. Specimens with this kind of failure mode exhibited stable and ductile characteristics up to ultimate deformation, and their maximum story drifts were
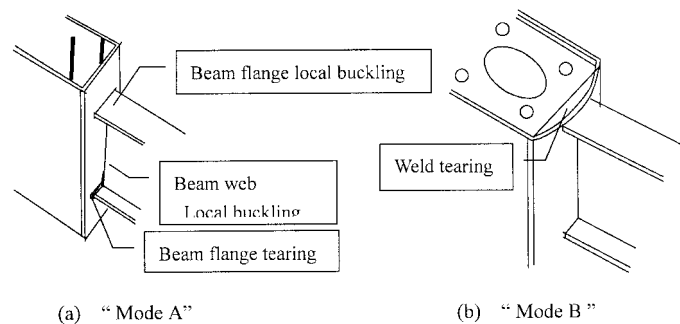


(a)  " Mode A"                                    (b)  " Mode B "

Fig. 2 Failure modes

Table 3 Main test results

| Specimen No. | | Overall response At Maximum strength | | | | Beam behavior | | |
|---|---|---|---|---|---|---|---|---|
| | | | | | | Yield | Ultimate | |
| | | $Q_{cm}^e$ (kN) | $R_{tm}$ ($10^{-3}$ rad) | $R_{tma}$ ($10^{-3}$ rad) | Failure Mode | $Q_{by}^e$ (kN) | $Q_{bm}^e$ (kN) | $R_{bm}^e$ ($10^{-3}$ rad) |
| YG1 | + | 96.7 | 31.3 | 35.1 | "B" | 48.8 | 59.8 | 23.4 |
| | − | 90.3 | 22.4 | 26.7 | | 48.5 | 55.8 | 12.6 |
| YG2 | + | 111.6 | 17.5 | 19.2 | "B" | 52.5 | 69.0 | 13.2 |
| | − | 107.3 | 19.0 | 20.1 | | 49.7 | 66.3 | 14.5 |
| YG3 | + | 113.2 | 34.3 | 41.0 | "A" | 48.2 | 70.0 | 24.8 |
| | − | 114.8 | 32.2 | 39.3 | | 49.4 | 71.0 | 22.9 |
| YG4 | + | 112.6 | 33.9 | 38.3 | "A" | 48.1 | 69.6 | 26.1 |
| | − | 125.0 | 39.0 | 42.5 | | 47.0 | 77.3 | 30.0 |
| YG5 | + | 117.6 | 40.0 | 44.8 | "A" | 48.9 | 72.7 | 29.6 |
| | − | 114.4 | 27.2 | 33.1 | | 48.3 | 70.7 | 20.7 |

Note: *$R_{tma}$ comes from the synthesized hysteresis curve (Kato 1982) and $Q_{by}^e$ from the synthesized curve by the general yield point method (Morita *et al.* 1992); superscript *e* is for the experimental value.

over 3%, which is larger than that of ordinary reinforced concrete structures. After tests, the column wall was removed from the concrete core in the region around the connection. No crushing of the concrete was found, and the tube wall did not display apparent outward signs of being overstressed.

The two collapse modes, denoted as either Mode "A", which includes the local buckling of beam flange and beam web, or "Mode B", which includes the tearing of the welding in the inner diaphragm respectively, are shown in Fig. 2. As described above, specimen YG1 and YG2 exhibited the failure mode "B" while specimen YG3, YG4 and YG5 exhibited the failure mode "A". It was expected that all of the specimens would fail in mode "A", since they were all designed with good ductility under seismic loading. However, the difficulty in inner diaphragm welding and the poor welding quality itself made the joint lose its capacity too early to achieve satisfactory results in mode "B". The main test results are outlined in Table 3, in which $R_{tma}$ comes from the synthesized hysteresis curve (Ben 1982), $Q_{by}^e$ from the synthesized curve by the general yield point method (Morita 1992), and superscript *e* is for the experimental value.
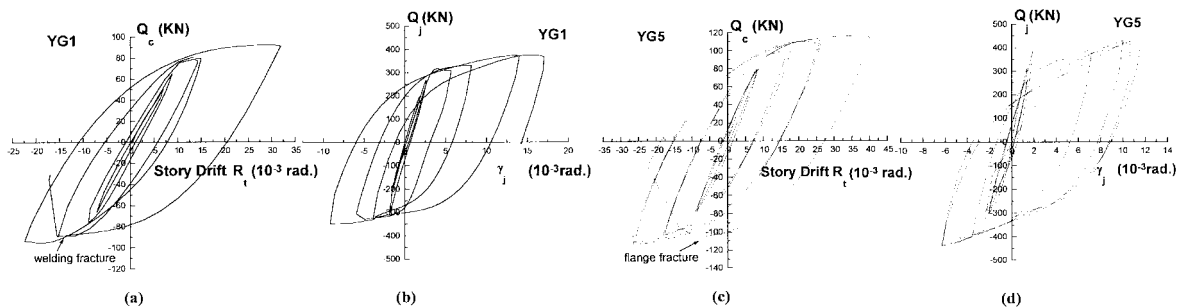


Fig. 3 Typical hysteresis curves of the specimens

*2.2.2. Load-deformation hysteresis curves*

Fig. 3 shows the typical hysteresis curves of the story shear force ($Q_c$) versus story drift rotation ($R_t$) and the shear force in the joint panel ($Q_j$) versus shear deformation ($\gamma_j$) for specimens YG1 and YG5. From Fig. 3 the following important facts are observed: the hysteresis curves of $Q_c$–$R_t$ for all the specimens are in a spindle shape; and specimen YG5 failed in failure Mode A, and attained a maximum strength at $R_{tm}=24\sim40\times10^{-3}$ rad. Since the test structure with steel beams rigidly framed into CFRT column has enough load bearing capacity and exhibits stable hysteresis characteristics with good ductility if a higher welding quality is guaranteed, it is suitable to be used in seismic regions. In order to observe the principles of stronger joint panel, weaker members, it is important for the joint panel to have enough load resistant capacity and stiffness. The $Q_j$–$\gamma_j$ hysteresis curves reveal that as the load increases, the stiffness of the $Q_j$–$\gamma_j$ hysteresis curves is degraded for all of the specimens. Among the 5 specimens, the degradation of stiffness for specimen YG1 is the most apparent, which can be explained by the fact that the infilled concrete can considerably improve the shear stiffness of the joint panel. Because the column wall thickness of YG3 is larger than that of YG4 and YG5, the degradation of stiffness for YG3 is slower than that of the latter two specimens. In addition, it can be concluded that the joint panels of the five specimens reached their yield strength from both the $Q_j$–$\gamma_j$ curves and the measured strain values.

# 3. Strength for the connection between the CFRT column and the steel beam

## 3.1. Yield and ultimate strength for the steel beam

The yield strength $Q^c_{by}$ and ultimate strength $Q^c_{bu}$ of the steel beam can be calculated simply by using the mechanics of materials and structures as follows:

$$Q^c_{by}=M_{by}/L_b=\{B_b \cdot t_{bf} (H_b - t_{bf}) \cdot f_{by} + (H_b - 2t_{bf})^2 \cdot t_{bw} \cdot f_{wy}/4\}/L_b \tag{1}$$

$$Q^c_{bu}=M_{bu}/L_b=\{B_b \cdot t_{bf} (H_b - t_{bf}) \cdot f_{bu} + (H_b - 2t_{bf})^2 \cdot t_{bw} \cdot f_{wy}/4 \}/L_b \tag{2}$$

Where $M_{by}$, $M_{bu}$ are the yield and ultimate moment capacity of the steel beam, respectively, $f_{by}$, $f_{bu}$ are the yield and ultimate strength of the steel beam flange, respectively, and $f_{wy}$ is the yield strength of the steel beam web. $L_b$ refers to Fig. 1, and the other symbols to Table 1.

## 3.2. Yield strength for the beam-to-column connection

The structural behavior of the connections between the CFRT column and the steel beam has been studied through the tensile tests of cruciform joint models with an inner diaphragm (Yu and Lu 1999). The formula for predicting the yield capacity of the connection are presented herein, which are based on the yield line theory, with the strain behavior of the connections taken into consideration. The yield mechanism of the connection is shown in Fig. 4.

The expression for yield strength of the beam to column connection, $P_p$, is as follows:

$$P_P = P_c + P_j = (4X + 2t)(M_p + M_a)/B_1 + 4B_cM_P/X + \sqrt{2}t_jf_y(h_2 + h_1/2) \tag{3}$$

where, $M_p$ is the yield moment of unit length in the column wall, $M_p=f_yt_{cf}^2/4$, $M_a$ is the yield
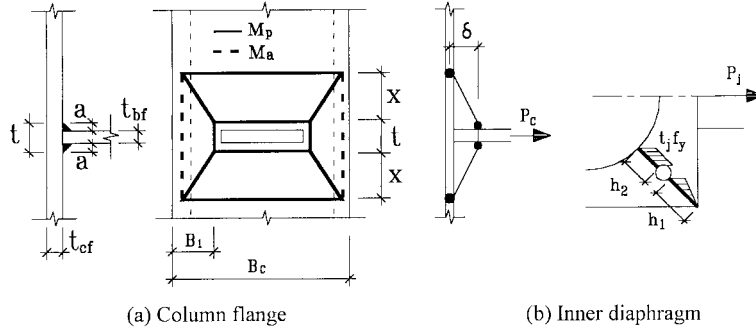
(a) Column flange        (b) Inner diaphragm

Fig. 4 Yield mechanism of the connection

moment of unit length in corner welding disregarding the effect of shear stress, $M_a = \min(M_p, f_y a^2/4)$, $a$ is the welding height and $f_y$ is the material yield point of the welded metal in corner seam. Unknown factor $X$ in Fig. 4 is the tension affected height which can be determined by the condition of minimizing the solution $P_p$, i.e., $\partial P_p/\partial X=0$, and in the present case, $X=\sqrt{B_1 B_c/2}$, where $B_1$, $B_1=(B_c-B_b-2a)/2$, and $B_c$, the column section width, are the geometric parameters, as shown in Fig. 4.

## 3.3. Yield strength for joint panel of the connection

The yield mechanism of the joint panel is assumed as shown in Fig 5. Based on the principle of virtual work, the following expression is obtained for the yield strength of joint panel (Morita *et al.*):

$$Q_{jy}H_b\theta=2M_c\theta-Q_bh_c\theta=2N_yh_c\theta+4M_{pw}\theta+4M_{pj}\theta+N_{cv}h_c\theta/2 \tag{4}$$

Where,

$$N_y=a\cdot H_b\cdot\tau_{ay}\approx a\cdot H_b\cdot f_{ay}/\sqrt{3}$$

$$M_{pw}=H_b^2\cdot t_{cf}\{1-\cos(\sqrt{3}h_c/H_b)\}f_{cy}/6$$

$$M_{pj}=h_ct_j^2f_{jy}/4 \tag{5}$$

$$N_{cv}=2h_c^2\cdot f_c/\{4+(h_c/H_b)^2\}$$



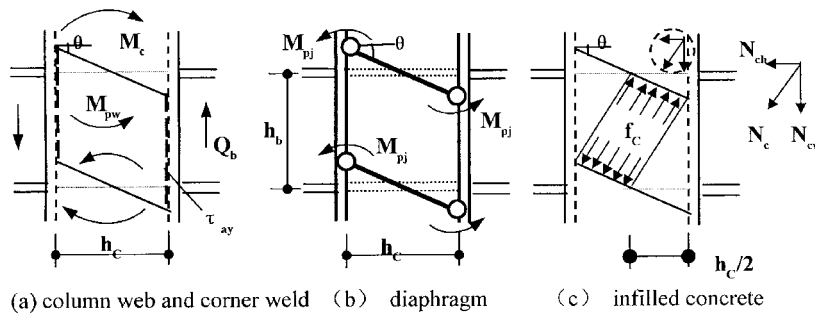(a) column web and corner weld    (b) diaphragm    (c) infilled concrete

Fig. 5 Yield mechanism of the joint panel

Thus, the yield strength of the joint panel is

$$Q_{jy} = (2N_y h_c + 4M_{pw} + 4M_{pj} + N_{cv} h_c / 2) / H_b \qquad (6)$$

### 3.4. Comparison of predicted strength with existing test results

In order to verify the proposed formula for the strength of the connection between CFRT column and steel beams, comparisons with existing test results were made and now presented in

Table 4 Comparison between predicted and tested strength of the beam

| No. | Direction | Yield | | | | Ultimate | | Remarks |
|-----|-----------|-------|-------|-------|-------|-------|-------|---------|
| | | $Q^e_{by}$ (kN) | $Q^c_{by}$ (kN) | $\dfrac{Q^e_{by}}{Q^c_{by}}$ | $Q^e_{bm}$ (kN) | $Q^c_{bu}$ (kN) | $\dfrac{Q^e_{bm}}{Q^c_{bu}}$ | |
| SPNO.4 | + | 373 | | 1.04 | 536 | | 1.01 | |
| | − | 373 | | 1.04 | 549 | | 1.03 | |
| SPNO.5 | + | 382 | 359 | 1.07 | 537 | 531 | 1.01 | (Sasaki *et al.* 1995) |
| | − | 373 | | 1.04 | 558 | | 1.05 | |
| SPNO.6 | + | 373 | | 1.04 | 526 | | 0.99 | |
| | − | 382 | | 1.07 | 522 | | 0.98 | |
| SPNO.1 | + | 319 | | 1.08 | 432 | | 0.99 | |
| | − | 319 | | 1.08 | 438 | | 1.01 | |
| SPNO.2 | + | 309 | 295 | 1.04 | − | 437 | − | (Teraoka & Morita 1994) |
| | − | 309 | | 1.04 | − | | − | |
| SPNO.3 | + | 319 | | 1.08 | 442 | | 1.02 | |
| | − | 319 | | 1.08 | 442 | | 0.95 | |
| YG1 | + | 48.8 | | 1.01 | 59.8 | | 0.85 | |
| | − | 48.5 | | 1.00 | 55.8 | | 0.79 | |
| YG2 | + | 52.5 | | 1.08 | 69.0 | | 0.98 | |
| | − | 49.7 | | 1.03 | 66.3 | | 0.94 | |
| YG3 | + | 48.2 | 48.4 | 1.00 | 70.0 | 70.3 | 1.00 | (The authors) |
| | − | 49.4 | | 1.02 | 71.0 | | 1.01 | |
| YG4 | + | 48.1 | | 0.99 | 69.9 | | 0.99 | |
| | − | 47.0 | | 0.97 | 77.3 | | 1.10 | |
| YG5 | + | 48.9 | | 1.01 | 72.7 | | 1.03 | |
| | − | 48.3 | | 1.00 | 70.7 | | 1.01 | |
| PS1 | + | 356 | | 1.10 | 476 | | 1.15 | |
| | − | 334 | | 1.03 | − | | − | |
| PS2 | + | 321 | | 0.99 | 440 | | 1.06 | |
| | − | 330 | 323 | 1.02 | − | 412 | − | (Morita *et al.* 1992) |
| PS3 | + | 302 | | 0.93 | − | | − | |
| | − | 297 | | 0.91 | 401 | | 0.97 | |
| PS4 | + | 318 | | 0.98 | − | | − | |
| | − | 317 | | 0.98 | 423 | | 1.03 | |

Note: superscript *e* is for experimental value, superscript *c* for calculated value, $Q^c_{by}$ and $Q^c_{bu}$ are calculated by Eq. (1) and Eq. (2) respectively.

Table 5 Comparison between predicted and tested strength of the beam-column connection

| Specimen NO. | Direction | Yield | | | Remarks |
|---|---|---|---|---|---|
| | | $Q_{py}^e$ (kN) | $Q_{py}^c$ (kN) | $\dfrac{Q_{py}^e}{Q_{py}^c}$ | |
| SPNO.4 | + | 368 | 398 | 0.92 | |
| SPNO.5 | + | 343 | 386 | 0.89 | (Sasaki *et al.* 1995) |
| SPNO.6 | + | 422 | 427 | 0.98 | |
| SPNO.1 | + | 363 | 378 | 0.96 | |
| SPNO.2 | + | 279 | 271 | 1.03 | (Teraoka & Morita 1994) |
| SPNO.3 | + | 323 | 340 | 0.95 | |
| NO.1 | + | 412 | 448 | 0.98 | (Teraoka 1991) (for the steel beams, |
| NO.2 | + | 319 | 298 | 1.07 | the effective width of upper flange is |
| NO.3 | + | 378 | 384 | 0.88 | 1.12 times of that of lower flange) |

Note: superscript *e* is for the experimental value, superscript *c* for the calculated value, $Q_{py}^c=P_p h_b/L_b$ and $P_p$ is calculated by Eq. (3).

Table 6 Comparison between predicted and tested strength of joint panel

| Specimen NO. | Direction | Yield | | | Remarks |
|---|---|---|---|---|---|
| | | $Q_{jy}^e$ (kN) | $Q_{jy}^c$ (kN) | $\dfrac{Q_{jy}^e}{Q_{py}^c}$ | |
| SPNO.4 | + | 2697 | 2430 | 1.11 | |
| SPNO.5 | + | 2434 | 2253 | 1.08 | (Sasaki *et al.* 1995) |
| SPNO.6 | + | 2844 | 3160 | 0.90 | |
| YG1 | + | 285 | 262 | 1.08 | |
| YG2 | + | 388 | 401 | 0.96 | |
| YG3 | + | 391 | 425 | 0.92 | The authors |
| YG4 | + | 367 | 348 | 1.05 | |
| YG5 | + | 383 | 372 | 1.03 | |
| NO.1 | + | 2275 | 2420 | 0.94 | |
| NO.2 | + | 1638 | 1516 | 1.08 | (Teraoka 1991) |
| NO.3 | + | 2128 | 2445 | 0.87 | |

Note: superscript *e* is for the experimental value, superscript *c* for the calculated value, and $Q_{jy}^c$ is calculated by Eq. (6).

Table 4, Table 5 and Table 6. Table 4 shows that Eq. (1) and Eq. (2) can accurately predict the yield and ultimate strength of the steel beams. Comparisons of the calculated yield strength to the measured one for beam-to-column connection and joint panel are shown in Table 5 and Table 6 respectively. It can be found that the calculated values are in good agreement with the measured ones and that the ratio of $Q_{py}^e/Q_{py}^c$ is in the range from 0.88 to 1.07 while $Q_{jy}^e/Q_{jy}^c$ is in the range from 0.87 to 1.11. Because the current available test data and parameters can not cover the full range in the typical construction of CFRT structures, further tests are still needed to verify the proposed formula.

## 4. Conclusions

Through the tests on the sub-assemblage specimens, the concluding remarks can be obtained as follows:

1) The test structures with steel beams rigidly framed into CFRT column had a good enough load bearing capacity and also exhibited stable hysteresis characteristics, good ductility and energy-absorbing capacities if the higher welding quality is guaranteed. Thus, this kind of connection is suitable to be used in seismic regions.

2) Formulas for predicting the yield capacity of the joint panel were obtained under the assumption of a simple stress transfer mechanism, with the infilled concrete taken into consideration. The calculated yield capacity agreed with the measured one.

3) Comparisons of the predicted strength to the tested data so far available show that they are in good agreement. However more test data and further studies are still needed in order to apply these formulas to engineering practice.

## References

Ben, Kato (1982), "Beam-to-column connection research in Japan," *Journal of Structural Division, ASCE*, **108**, 343-360.

Koji, Morita, Kazumasa Ebato *et al.*, "Study on structural behaviors of beam-to-column connection in case corner weld of box column", *Journal of Structural and Construction Engineering, AIJ*, 397, 48-59 (in Japanese).

Koji, Morita, Masaru Teraoka and Takahiko Suzuki (1992), "Experimental study on connections between concrete filled square tubular high strength (780MPa) steel column and H-beam," *Proceedings of 3rd Pacific Structural Steel Conference*, Oct., 591-598.

Masaru, Teraoka, Koji Morita (1991), "Structural design of high rise building consists of concrete filled square tubular column and steel composite beams and its experimental verification", *Tubular Structures 4th International Symposium*, Delft, 392-401.

Masaru, Teraoka, Koji Morita (1994), "Experimental study on structural behavior of concrete filled square tubular column to steel beam connections without diaphragm", *Proceedings of the 4th ASCCS International Conference*, 190-193.

Saito, Hideto and Saito, Hikaru (1994), "Fire resistance of concrete filled steel tube columns", *Journal of Structural and Construction Engineering, AIJ*, **458**, April, 163-169 (in Japanese).

Satoshi, Sasaki, Masaru, Teraoka, Koji, Morita and Toshio, Fujiwara (1995), "Structural behavior of concrete filled square tubular column with partial penetration weld corner seam to steel H-beam connection", *Proceedings of the 4th Pacific Structural Steel Conference*, **4**(2), October, 33-40.

Tie, T.T. (1996), "Fire resistance of steel columns filled with bar-reinforced concrete", *Journal of Structural Engineering, ASCE*, **122**(1), 30-36.

Yu, Yong, Lu, Xilin, *et al.* (1999), "Experimental study on connection between concrete-filled square tube column and steel beams under tensile loading", *Structural Engineer,* **48**, 23-28 (in Chinese).